Evolution of the Crystal and Electronic Structures of Magnetic $RuSr_{2-x}La_xGdCu_2O_8$ Superconductors upon La Substitution

Su Gil Hur, Dae Hoon Park, and Seong-Ju Hwang*

Division of Nano Sciences and Department of Chemistry, Ewha Womans University, Seoul 120-750, Korea

Seung Joo Kim

Department of Chemistry, College of Natural Sciences, Ajou University, Gyunggi 443-749, Korea

J. H. Lee and Sang Young Lee

Department of Physics and Department of Advanced Technology Fusion, Center for Emerging Wireless Transmission Technology, Konkuk University, Seoul 143-701, Korea

Received: November 26, 2004; In Final Form: March 14, 2005

We have investigated systematically the effects of La substitution on the chemical bonding nature and physical properties of magnetic $RuSr_{2-x}La_xGdCu_2O_8$ superconductors. X-ray diffraction and energy dispersive spectroscopic microprobe analyses reveal that a fraction of Sr ions can be successfully replaced by La ions with the contraction of unit cell volume. According to electrical resistance and dc magnetization measurements, the La substitution gives rise to a significant reduction of superconducting transition temperature (T_c) but to an increase of magnetic ordering temperature with depressed remanent magnetization. Ru K- and Cu K-edge X-ray absorption spectroscopic results clarify that average Ru and Cu oxidation states decrease upon the La substitution. On the basis of the spectroscopic evidences presented here, we are able to attribute the T_c reduction upon the La substitution to the depletion of the hole density in CuO_2 layers and the accompanying variation of magnetic coupling behavior to the change of Ru oxidation state.

Introduction

The discovery of the coexistence of ferromagnetism and superconductivity in ruthenocuprates $RuSr_2LnCu_2O_8$ (Ln = Gd, Eu) has evoked intense research interest, since it can provide an opportunity for understanding the effects of intrinsic magnetic field on the superconducting properties of layered copper oxides.[1−3] Over the past decade, there have been many research activities performed on the physicochemical properties of these magnetic superconductors, which include spin alignment and interaction, superconductivity, crystal and electronic structures, and so on.[3−14] Especially the magnetic structure of the compounds was intensively investigated by using various physical and spectroscopic tools.[3,6−11] However, some controversies still exist over the type of the magnetic order in the RuO_2 layer. For instance, there are reports on ferromagnetic order of the Ru moments[6] and antiferromagnetic alignment of the Ru moments along the *ab*-plane and the *c*-axis.[7,8] On the other hand, the field dependence of the magnetic susceptibility strongly suggests that the magnetic moments are predominantly of antiferromagnetic order with a small ferromagnetic component.[8,9] Moreover, the mixed oxidation states of Ru ions make it more difficult to understand the nature of magnetic coupling in this material.[10] On the basis of neutron diffraction data and the first-principle calculation,[7,8] the presence of a weak ferromagnetism was postulated due to the canting of antiferromagnetically ordered Ru moments, which originates from the tilting of the RuO_6 octahedra. Such a canted ferromagnetic alignment of the Ru moments would induce a pair breaking effect in the superconductive CuO_2 layer. In this context, some experimental and theoretical studies have been performed for understanding the influence of ferromagnetism on superconductivity. However, the interplay between intrinsic magnetic field and superconductivity has remained unclear. Moreover, some contradictory results exist on the hole doping state of this material.[11−14] According to valence bond sum calculation based on the structural data of $RuSr_2GdCu_2O_8$,[11] this compound possesses an overdoped hole concentration of ∼0.4. On the contrary, studies on thermoelectric power have indicated the existence of underdoped hole density in $RuSr_2GdCu_2O_8$.[12,13] From Ru L_{III}-edge X-ray absorption spectroscopic (XAS) analysis,[14] the hole density of CuO_2 in $RuSr_2GdCu_2O_8$ was estimated to be ∼0.20, indicating that this compound is in an optimally hole doping region.

To address the above-mentioned problems, we have synthesized and characterized La-substituted $RuSr_{2-x}La_xGdCu_2O_8$ ruthenocuprates, since the aliovalent substitution of Sr^{+II} with La^{+III} allows us to control the hole density of the CuO_2 layer and the magnetic coupling of the RuO_2 layer. Despite several reports on cation-substituted $RuSr_2GdCu_2O_8$ systems,[15−19] only a few attempts have been made to probe the effects of chemical substitution on the electronic and crystal structures of the ruthenocuprate. Such an investigation can provide crucial insight for the superconducting and magnetic properties of this phase. In this context, we have applied Cu K- and Ru K-edge X-ray absorption near edge structure (XANES) analyses for the La-substituted ruthenocuprates in order to probe the effect of La substitution on the average oxidation states of Cu and Ru ions.

* To whom correspondence should be addressed. Phone: +82-2-3277-3420. Fax: +82-2-3277-3419. E-mail: hwangsju@ewha.ac.kr.

10.1021/jp044611f CCC: $30.25
Published on Web 04/15/2005

Also, variations in the crystal structure upon the lanthanum substitution have been investigated by using X-ray diffraction (XRD) and extended X-ray absorption fine structure (EXAFS) techniques.

Experimental Section

The polycrystalline samples of $RuSr_{2-x}La_xGdCu_2O_8$ ($x = 0$ and 0.1) were synthesized by the conventional solid state reaction method, as reported previously.[4] For preparing single-phase materials without the ferromagnetic $SrRuO_3$ phase, we applied a preliminary calcination step in flowing argon, which was followed by prolonged sintering procedures for more than 3 weeks in an oxygen atmosphere with intermittent grindings. The formation of pure ruthenocuprates and the variation of lattice parameters were examined by XRD measurements using Ni filtered Cu Kα radiation with a graphite diffracted beam monochromator. The morphology and particle size of the samples were determined by scanning electron microscopy (SEM) using a JEOL JSM-6700F microscope. During SEM experiments, semiquantitative energy dispersive spectroscopic (EDS) microprobe analysis was also carried out on several crystallites to confirm the incorporation of La into the ruthenocuprate lattice. Variations in the electrical conduction and magnetic coupling upon the La substitution were probed by performing resistance and dc magnetization measurements, respectively. XAS experiments were carried out at Cu K- and Ru K-edges by using the EXAFS facility installed at the beam line 7C at the Pohang Light Sources (PLS) in Korea. XAS data were collected at room temperature in a transmission mode using gas-ionization detectors. All the present spectra were calibrated carefully by measuring the spectra of the Cu metal or RuO_2 reference. Data analysis for the experimental spectra was performed by using the standard procedure reported previously.[20] In the course of EXAFS fitting analysis, the coordination number (CN) was fixed to the crystallographic values while the amplitude reduction factor (S_0^2) was allowed to vary. Also, all the bond distances (R), Debye−Waller factors (σ^2), and energy shifts (ΔE) were set as variables. Due to the limitation in the numbers of allowed variables, we have kept the energy shift the same for two (Cu−O) shells at ~1.90−2.20 Å and two (Ru−O) shells at ~1.91−1.97 Å. Such constraints can be rationalized from the fact that the adjacent shells consisting of the same types of atoms would possess a very similar degree of energy shift.

Results and Discussion

Powder XRD patterns of the lanthanum-substituted $RuSr_{2-x}La_xGdCu_2O_8$ ($x = 0$ and 0.1) are presented in Figure 1. All the diffraction peaks match well with the simulated pattern of layered perovskite structure with the tetragonal symmetry.[4] There is no reflection corresponding to the ferromagnetic $SrRuO_3$ phase, indicating the formation of a pure ruthenocuprate phase. According to least-squares fitting analyses, the c-axis lattice parameter decreases upon the La substitution, whereas the in-plane lattice parameter becomes greater.[21] The unit cell volume decreases by replacing a fraction of strontium ions with lanthanum ions, which is due to the smaller size of the latter compared to the former ($Sr^{+II}(12) = 1.58$ Å and $La^{+III}(12) = 1.50$ Å, where the number in parentheses represents the coordination number).[22]

We have examined the morphology and particle size of the ruthenocuprates by using SEM. As shown in Figure 2, both unsubstituted and La-substituted compounds display platelike morphology having a stack of layered crystallites. Such a crystal

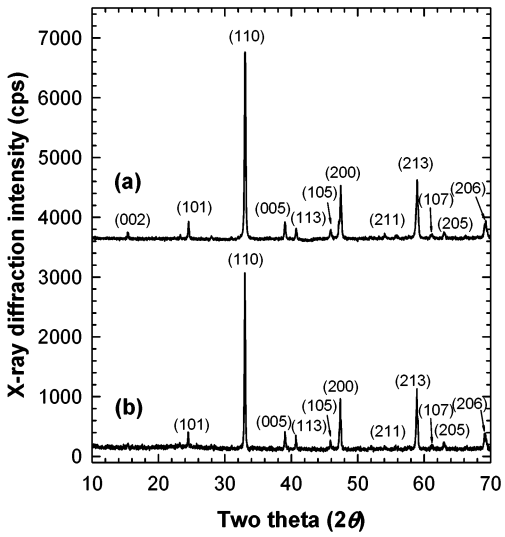

Figure 1. Powder XRD patterns for the lanthanum-substituted $RuSr_{2-x}La_xGdCu_2O_8$ with $x = 0$ (a) and 0.1 (b). The pattern of the unsubstituted compound is shifted upward by 3500 cps for easier comparison.

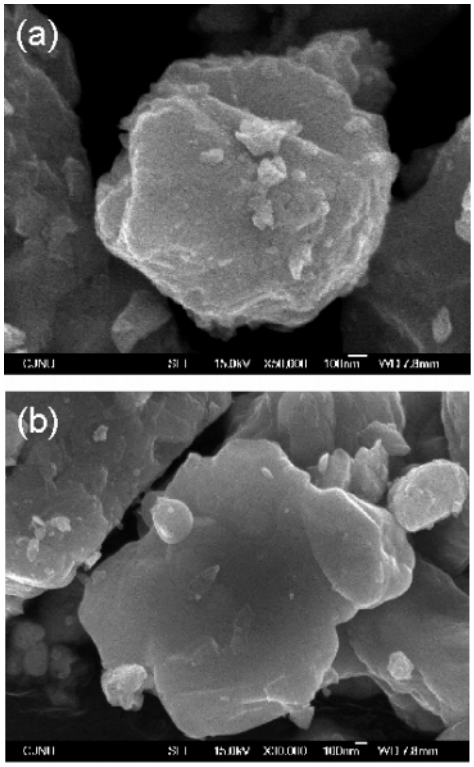

Figure 2. SEM images for the lanthanum-substituted $RuSr_{2-x}La_xGdCu_2O_8$ with $x = 0$ (a) and 0.1 (b).

shape would originate from the high structural anisotropy of the ruthenocuprates. The particle size of both compounds ranges from ~1−5 μm, indicating little influence of the La substitution on the crystal growth. The partial replacement of Sr by La was ensured from EDS analysis.

The normalized electrical resistivity of $RuSr_{2-x}La_xGdCu_2O_8$ ($x = 0$ and 0.1) was measured as a function of temperature to probe the effect of the La substitution on the superconducting properties of the ruthenocuprates. As shown in Figure 3, the critical onset temperature ($T_{c,on}$) and zero-resistance temperature ($T_{c,zero}$) are 50.1 and 31.8 K, respectively, for the pristine compound ($x = 0$). Meanwhile, abrupt changes in $T_{c,on}$ and $T_{c,zero}$ are observed for $x = 0.1$, with corresponding values of 15.0

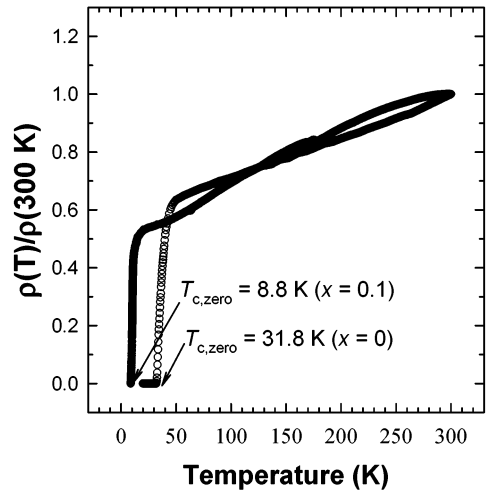

Figure 3. Normalized electrical resistivity $\rho(T)/\rho(300\ K)$ vs temperature plot for $RuSr_{2-x}La_xGdCu_2O_8$ with $x = 0$ (open) and 0.1 (filled). Here, $\rho(T)$ and $\rho(300\ K)$ denote the electrical resistivity at the measured temperature (T) and at 300 K, respectively.

and 8.8 K for the La-substituted derivative. The significant change in T_c upon the partial substitution of La for Sr suggests that variations in the fundamental properties of $RuSr_{2-x}La_xGdCu_2O_8$ on x are significant near $x = 0$, emphasizing the importance of controlling x for studying the effects of the La substitution. In Figure 3, the electrical properties of $RuSr_{1.9}La_{0.1}GdCu_2O_8$ appear as rather metallic as $RuSr_2GdCu_2O_8$ with almost linear temperature dependence of the resistivity at temperatures higher than the onset critical temperature.

To probe the effect of the La substitution on the magnetic coupling behaviors of the ruthenocuprate, we have measured hysteresis loops of dc magnetization at various temperatures of 5−160 K. Even though only the data at 5, 80, and 160 K are presented in Figure 4 for clarity, we have found that both compounds exhibit a magnetic irreversibility below 130 K indicative of weak ferromagnetism. In the case of the magnetization data recorded at 160 K, only the La-substituted derivative displays a weak hysteresis that is absent for the unsubstituted compound. This observation underlines the increase of magnetic ordering temperature upon the La substitution.[18] A closer inspection on the magnetization data unfolds the lowering of the coercive field (H_{co}) and remanent magnetization (M_r) at 5 K upon the La substitution: $H_{co} \cong 410$ Oe and $M_r \cong 0.17\ \mu_B$/formula unit for the pristine compound and $H_{co} \cong 230$ Oe and $M_r \cong 0.07\ \mu_B$/formula unit for the La-substituted derivative. This finding suggests a slight decrease of the weak ferromagnetic component after the La substitution, which is in good agreement with the previous report.[18] It is worthwhile to note here that temperature dependent magnetic susceptibility data (not shown) display a small upturn of magnetic susceptibility below 20 K for both the samples, indicating the presence of a ferromagnetic impurity phase. The absence of any distinct impurity peaks in the corresponding XRD patterns suggests a very low concentration of this ferromagnetic phase, if any (Figure 1). Moreover, the contribution of this secondary phase to the low temperature magnetization data appears to be similar in magnitude for both the samples. In this regard, we are able to conclude that, despite the existence of a small amount of the ferromagnetic phase, the La substitution surely leads to a depression of the weak ferromagnetic component of the Ru-based cuprate.

For a better understanding of variations in the superconducting and magnetic properties upon the La substitution, we have

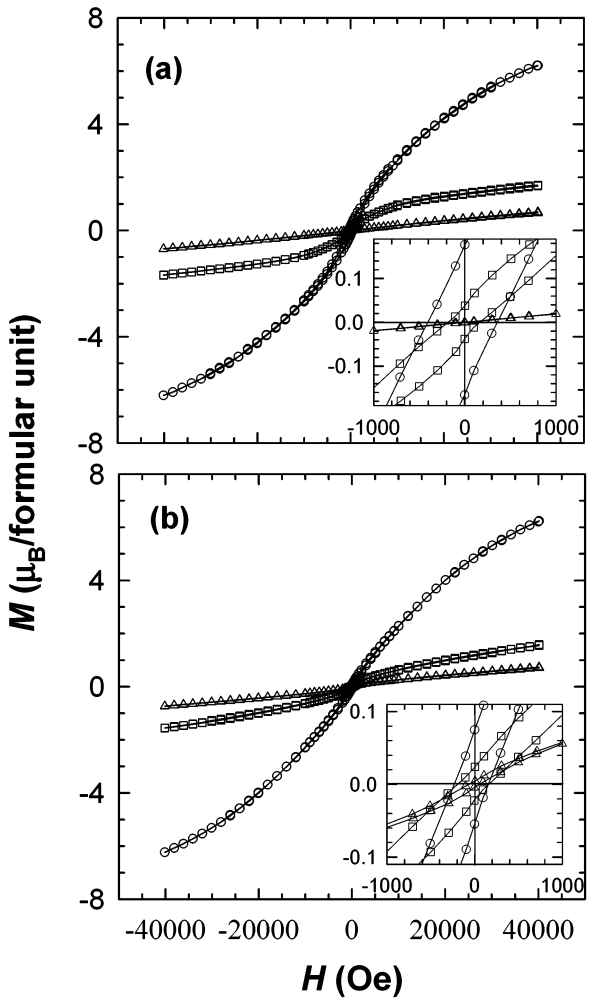

Figure 4. Magnetization (M) vs applied field (H) plots for $RuSr_{2-x}La_xGdCu_2O_8$ with $x = 0$ (a) and 0.1 (b). The circles, squares, and triangles represent the magnetization data measured at 5, 80, and 160 K, respectively. Inset: enlarged views of M vs H plots for an applied field range of −1000 to +1000 Oe.

investigated the electronic structure and local atomic arrangement of $RuSr_{2-x}La_xGdCu_2O_8$ by using XAS analyses at Cu K- and Ru K-edges. The Cu K-edge XANES spectra for $RuSr_{2-x}La_xGdCu_2O_8$ ($x = 0$ and 0.1) are presented in Figure 5, together with those for references $La_2Cu^{+II}O_4$, $Nd_2Cu^{+II}O_4$, and $LaCu^{+III}O_3$ where the divalent or trivalent copper ion is in different local geometries. The edge energies of the ruthenocuprates appear lower than that of the Cu^{+III} reference, while they appear slightly higher than those of the Cu^{+II} references, indicating the existence of a mixed oxidation state of copper (Cu^{+II}/Cu^{+III}) in the ruthenocuprates. However, the presence of several fine features near edge jump makes it difficult to quantitatively determine the Cu oxidation state from the degree of edge shift. As shown in the figure, a small pre-edge peak (P) appears commonly for all the compounds under investigation, which is due to the quadruple-allowed transition from the core 1s level to an unoccupied 3d state.[23] The position of this peak provides an effective measure for the oxidation state of copper quantitatively. As can be seen clearly from the inset of Figure 5, an enhanced formal valence from Cu^{+II} to Cu^{+III} leads to an increase of the peak energy by 1.1−1.2 eV. In light of this, the average Cu oxidation state of $RuSr_2GdCu_2O_8$ was estimated to be $\sim +2.09$.[24] These findings can provide strong evidence for the existence of an underdoped hole density in the ruthenocuprate phase, which is supported by an observation of the significantly reduced

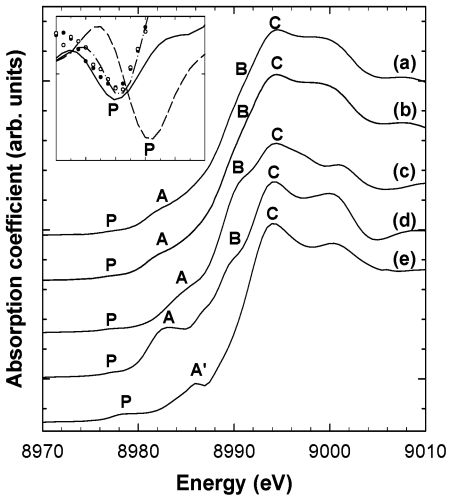

Figure 5. Cu K-edge XANES spectra for $RuSr_{2-x}La_xGdCu_2O_8$ with x = (a) 0 (open circles) and (b) 0.1 (closed circles), compared with those for (c) La_2CuO_4 (solid line), (d) Nd_2CuO_4 (dot−dashed line), and (e) $LaCuO_3$ (dashed line). The descriptions in parentheses are for the data in the inset. Inset: an enlarged view of the second derivative spectra for an energy range of 8975−8980 eV.

T_c after the La substitution. Also, a slight shift of the peak P toward the low energy side is discernible after the La substitution, suggestive of a decrease in the hole density. In the main-edge region, there are some features corresponding to the dipole-allowed transitions from the core 1s level to unoccupied 4p states, which are denoted by A (or A′), B, and C. According to a previous Cu K-edge XANES study,[23] the peaks A (or A′) and B are attributed to the transitions from the 1s orbital to the out-of-plane $4p_\pi$ one with and without the shakedown processes, respectively, while the peak C is ascribed to the transition to the in-plane $4p_\sigma$ orbital without the shakedown process. Among these features, the shakedown peak A reflects very sensitively the local crystal structure around copper,[23] since the presence of axial ligands hinders an effective shakedown process along the *c*-axis. Therefore, the most intense peak A occurs in the reference Nd_2CuO_4 without axial ligands. The present ruthenocuprates with CuO_5 square pyramidal units exhibit weaker intensity than the reference Nd_2CuO_4. In addition, the shakedown peak A′ around 8986 eV provides an indicator for the presence of trivalent copper ions, as in $LaCuO_3$.[25] As can be seen clearly from Figure 5, this feature is absent in the spectra of the present ruthenocuprates, cross-confirming the underdoped state of this material.

Local structural variations in the CuO_2 layer upon the La substitution were determined quantitatively by applying the Cu K-edge EXAFS technique. Figure 6a illustrates the Fourier transformed k^3-weighted Cu K-edge EXAFS spectra for the ruthenocuprate $RuSr_{2-x}La_xGdCu_2O_8$ (x = 0 and 0.1) in the k range 3.55−11.20 Å^{-1}. In the Fourier transform (FT) diagrams, the ruthenocuprates exhibit several intense FT peaks at ∼1.5, ∼2.9, and ∼3.7 Å, corresponding to Cu−O, Cu−Gd/Sr, and Cu−Ru/Cu shells, respectively. For quantitative analysis for the variation of the bond distances, the first and second FT peaks were isolated by inverse FT to k space. The resulting $k^3\chi(k)$ Fourier filtered EXAFS oscillations are presented in Figure 6b, and the curve fittings were carried out to determine the structural parameters such as the coordination number (CN), bond length (R), and Debye−Waller factor (σ^2). The best-fitted results are compared to the experimental spectra in Figure 6a and b, and the fitted structural parameters are listed in Table 1.[26] Upon the La substitution, the out-of-plane Cu−O_{ax} bond shows a significant elongation, which is greater than the error range for

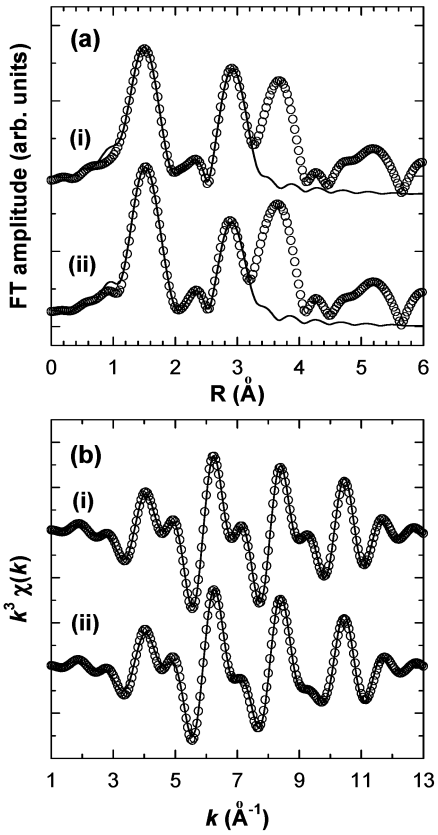

Figure 6. (a) Fourier transformed and (b) Fourier filtered Cu K-edge EXAFS data for $RuSr_{2-x}La_xGdCu_2O_8$ with x = 0 (i) and 0.1 (ii). The open circles and solid lines represent the experimental and calculated data, respectively.

TABLE 1: Results from a Nonlinear Least-Squares Fit for the Cu K-Edge EXAFS Spectra for $RuSr_{2-x}La_xGdCu_2O_8$ with x = 0 and 0.1, Respectively

sample	bond	CN	R (Å)	σ^2 (10^{-3} × Å^2)
$RuSr_2GdCu_2O_8$[a]	Cu−O_{eq}	4	1.91	5.13
	Cu−O_{ax}	1	2.23	5.48
	Cu−Gd	4	3.14	7.32
	Cu−Sr	4	3.23	15.99
$RuSr_{1.9}La_{0.1}GdCu_2O_8$[a]	Cu−O_{eq}	4	1.92	4.37
	Cu−O_{ax}	1	2.26	4.36
	Cu−Gd	4	3.13	9.65
	Cu−Sr/La	4	3.17	18.58

[a] The curve fitting was performed for the range 1.043 − R − 3.16 Å and 3.55 − k − 11.20 Å^{-1}.

the estimated bond length ($\Delta R \sim \pm 0.01$ Å). Such a variation in the crystal structure underlines the reduction of the CuO_2 layer due to an electron doping by the La substitution, which is well consistent with the red shift of the pre-edge peak position in the Cu K-edge XANES spectra (see Figure 5). However, the La substitution leads to shortening of the interatomic distance for distant shells such as Cu−Sr/La,[27] which would be ascribable to the accompanying lattice contraction and/or to the replacement of Sr^{+II} with La^{+III}.

The electronic configuration and crystal structure of the RuO_2 layer in $RuSr_{2-x}La_xGdCu_2O_8$ (x = 0 and 0.1) have also been studied by performing Ru K-edge XANES/EXAFS analysis. Figure 7 presents the Ru K-edge XANES spectra for $RuSr_2GdCu_2O_8$ and $RuSr_{1.9}La_{0.1}GdCu_2O_8$ as well as for the reference samples of $SrRu^{+IV}O_3$, $Ru^{+IV}O_2$, and $Sr_2Ru^{+V}{}_{0.5}Gd_{0.5}O_4$. The edge energies of the ruthenocuprates appear higher than those of Ru^{+IV} in $SrRu^{+IV}O_3$ and $Ru^{+IV}O_2$, while they appear slightly lower than that of Ru^{+V} in $Sr_2Ru^{+V}{}_{0.5}Gd_{0.5}O_4$. This energy

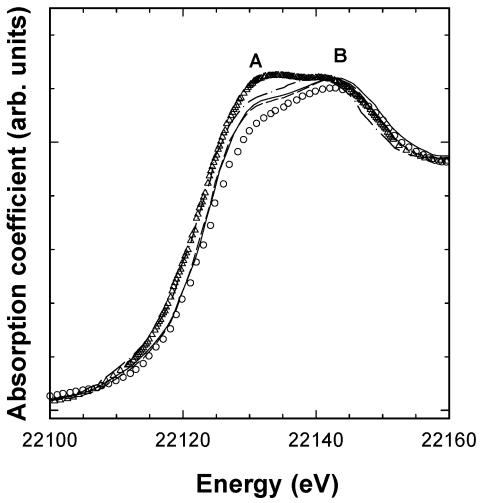

Figure 7. Ru K-edge XANES spectra for $RuSr_{2-x}La_xGdCu_2O_8$ with $x = 0$ (solid line) and 0.1 (dashed line), in comparison with those for the reference samples of $SrRuO_3$ (dot−dashed line), RuO_2 (triangles), and $SrRu_{0.5}Gd_{0.5}O_4$ (circles).

difference provides evidence for the mixed oxidation state of ruthenium (Ru^{+IV}/Ru^{+V}) in the compounds. Upon the La substitution, the position of edge jump shifts slightly toward the lower energy side, indicating the decrease of the Ru oxidation state. On the basis of the energy difference of edge jump between $SrRu^{+IV}O_3$ and $Sr_2Ru^{+V}{}_{0.5}Gd_{0.5}O_4$ ($\Delta E = 2.1$ eV), we are able to estimate the oxidation state of ruthenium as ~4.76 for $RuSr_2GdCu_2O_8$ and ~4.69 for $RuSr_{1.9}La_{0.1}GdCu_2O_8$. In consideration of a fixed oxygen content of the ruthenocuprate of 8,[4] the estimated Ru valence $\sim +4.8$ for $RuSr_2GdCu_2O_8$ matches well with the average Cu oxidation state $\sim +2.1$ calculated from Cu K-edge XANES results. This result highlights the role of the RuO_2 layer as a charge reservoir providing holes to the superconductive CuO_2 layer.

The FT data of Ru K-edge EXAFS spectra for the ruthenocuprate $RuSr_{2-x}La_xGdCu_2O_8$ ($x = 0$ and 0.1) and their inverse FT spectra are presented in parts a and b of Figure 8, respectively. There are two intense FT peaks at ~1.5 and ~3.1 Å in the FT data of the ruthenocuprates, which originate from Ru−O and Ru−Sr/La shells, respectively. To determine the variation of the bond distances of Ru−O, the first FT peak was isolated by inverse FT to k space and then curve fitted. The best fitting results are compared to the experimental spectra in Figure 8a and b, and the fitted structural parameters are summarized in Table 2.[28] The in-plane and out-of-plane Ru−O bonds show minute changes upon the La substitution such as a slight shortening of bond lengths. Although the observed change of bond distances may be within the error range of the EXAFS analysis, such a small variation of the $Ru-O_{ax}$ bond distance could be understood on the basis of a competing bond model, in which the elongation of the $Cu-O_{ax}$ bond upon the La substitution gives rise to the shrinkage of the competing $Ru-O_{ax}$ bond.

From the present experimental findings, it is evident that the Cu and Ru oxidation states in $RuSr_2GdCu_2O_8$ become diminished after the partial replacement of Sr with La. In this regard, the observed T_c reduction upon the La substitution is attributable to the hole depletion and provides evidence for the underdoped hole density in $RuSr_2GdCu_2O_8$. The Cu and Ru valences in $RuSr_{2-x}La_xGdCu_2O_8$ ($x = 0$ and 0.1) as determined by the XANES analysis support our arguments. On the other hand, we are able to explain the variation of magnetic ordering behaviors after the La substitution from the viewpoint of the

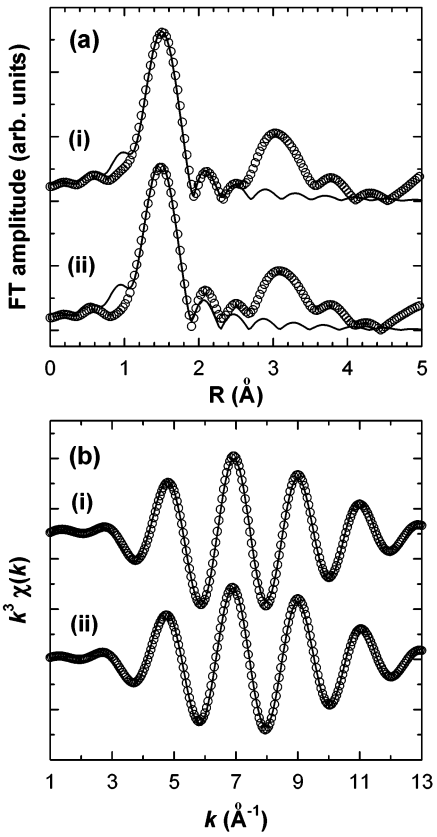

Figure 8. (a) Fourier transformed and (b) Fourier filtered Ru K-edge EXAFS data for $RuSr_{2-x}La_xGdCu_2O_8$ with $x = 0$ (i) and 0.1 (ii). The open circles and solid lines represent the experimental and calculated data, respectively.

TABLE 2: Results from a Nonlinear Least-Squares Fit for the Ru K-Edge EXAFS Spectra for $RuSr_{2-x}La_xGdCu_2O_8$ with $x = 0$ and 0.1, Respectively

sample	bond	CN	R (Å)	σ^2 ($10^{-3} \times$ Å^2)
$RuSr_2GdCu_2O_8$[a]	$Ru-O_{ax}$	2	1.92	1.68
	$Ru-O_{eq}$	4	1.98	3.28
$RuSr_{1.9}La_{0.1}GdCu_2O_8$[b]	$Ru-O_{ax}$	2	1.91	0.83
	$Ru-O_{eq}$	4	1.97	2.92

[a] The curve fitting was performed for the range $0.951 - R - 1.902$ Å and $4.20 - k - 12.05$ Å^{-1}. [b] The curve fitting was performed for the range $0.982 - R - 1.871$ Å and $4.15 - k - 12.00$ Å^{-1}.

change of Ru oxidation state. The decreased oxidation state of Ru in the La-substituted derivative implies the increased population of tetravalent Ru^{+IV} ions. Consequently, the magnetic coupling of the RuO_2 layer becomes rather similar to $SrRu^{+IV}O_3$ with a higher magnetic ordering temperature (~160 K) compared to $RuSr_2GdCu_2O_8$. Such a change of the bonding character of ruthenium ions would be responsible for the higher magnetic ordering temperature of the La-substituted derivative than the pristine compound. In fact, the increase of magnetic transition temperature caused by electron doping was previously reported for the $RuSr_2Gd_{1-x}Ce_xCu_2O_8$ system.[19] Besides, the depression of Ru oxidation state allows us to understand the decreased remanent magnetization of the La-substituted derivative, as follows. With reference to the preferred spin state of Ru ions in the perovskite-type compounds (i.e., $S = 1$ for Ru^{+IV} and $S = {}^3/_2$ for Ru^{+V}) and previous NMR studies on the ruthenocuprate,[29−32] it is highly feasible that the reduction of the Ru^{+V} ion by the La substitution lowers the overall magnetic moments of the RuO_2 layers. Judging from the previous Rietveld results revealing a negligible influence of the La substitution on the

canting angle of RuO_6 octahedra,[18] we can ascribe the lowered remanent magnetization of the La-substituted compound to the decrease of the Ru magnetic moments.

Conclusions

In this study, we have tried to understand the effects of lanthanum substitution on the superconducting and magnetic properties of ruthenocuprates $RuSr_{2-x}La_xGdCu_2O_8$ ($x = 0$ and 0.1). From the present XAS results, it becomes clear that the partial substitution of La for Sr causes a decrease of the Cu and Ru oxidation states. These effects allow us to explain the significant reduction in T_c and the change of magnetic coupling behaviors upon the La substitution. We have concluded that the ruthenocuprate phase has an underdoped hole density with the magnetic behavior of the RuO_2 layer being very sensitive to the average oxidation state of ruthenium.

Acknowledgment. This work was supported by Korea Research Foundation Grant (KRF-2003-042-C00065). The experiments at PLS were supported in part by MOST and POSTECH.

References and Notes

(1) Bauernfeind, L.; Wider, W.; Braun, H. F. *Physica C* **1995**, *254*, 151.

(2) Tallon, J. L.; Bernhard, C.; Bowden, M. E.; Gilberd, P. W.; Stoto, T. M.; Pringle, D. J. *IEEE Trans. Appl. Supercond.* **1999**, *9*, 1696.

(3) Williams, G. V. M.; Kramer, S. *Phys. Rev. B* **2000**, *62*, 4132.

(4) Chmaissem, O.; Jorgensen, J. D.; Shaked, H.; Dollar, P.; Tallon, J. L. *Phys. Rev. B* **2000**, *61*, 6401.

(5) Picket, W. E.; Weht, R.; Shick, A. B. *Phys. Rev. Lett.* **1999**, *83*, 3713.

(6) Bernhard, C.; Tallon, J. L.; Neidermayer, Ch.; Blasius, Th.; Golnik, A.; Brucher, E.; Kremer, R. K.; Noakes, D. R.; Stronach, C. E.; Ansaldo, E. J. *Phys. Rev. B* **1999**, *59*, 14099.

(7) Nakamura, K.; Freeman, A. J. *Phys. Rev. B* **2002**, *66*, 140405.

(8) Jorgensen, J. D.; Chmaissem, O.; Shaked, H.; Short, S.; Klamut, P. W.; Dabrowski, B.; Tallon, J. L. *Phys. Rev. B* **2001**, *63*, 054440.

(9) Lynn, J. W.; Keimer, B.; Ulrich, C.; Bernhard, C.; Tallon, J. L. *Phys. Rev. B* **2000**, *61*, R14964.

(10) Butera, A.; Fainstein, A.; Winkler, E.; Tallon, J. L. *Phys. Rev. B* **2001**, *63*, 054442.

(11) McLaughlin, A. C.; Zhou, W.; Attfield, J. P.; Fitch, A. N.; Tallon, J. L. *Phys. Rev. B* **1999**, *60*, 7512.

(12) Tallon, J. L.; Loram, J. W.; Williams, G. W. M.; Bernhard, C. *Phys. Rev. B* **2000**, *61*, R6471.

(13) Pozek, M.; Dulcic, A.; Paar, D.; Williams, G. V. M.; Kramer, S. *Phys. Rev. B* **2001**, *64*, 064508.

(14) Liu, R. S.; Jang, L. Y.; Hung, H. H.; Tallon, J. L. *Phys. Rev. B* **2001**, *63*, 212507.

(15) Tokunaga, Y.; Kotegawa, H.; Ishida, K.; Kitaoka, Y.; Takagiwa, H.; Akimitsu, J. *Phys. Rev. Lett.* **2001**, *86*, 5767.

(16) Ruiz-Bustos, R.; Gallardo-Amores, J. M.; Saez-Puche, R.; Moran, E.; Alario-Franco, M. A. *Physica C* **2002**, *382*, 395.

(17) Vecchione, A.; Gombos, M.; Pace, S.; Tedesco, C.; Zola, D. *Physica C* **2002**, *372*−*376*, 1229.

(18) Mandal, P.; Hassen, A.; Hemberger, J.; Krimmel, A.; Loidl, A. *Phys. Rev. B* **2002**, *65*, 144506. Hassen, A.; Mandal, P.; Hemberger, J.; Krimmel, A.; Choudhury, P.; Gosh, B.; Loidl, A. *Physica C* **2003**, *398*, 123.

(19) Klamut, P. W.; Dabrowski, B.; Mais, J.; Maxwell, M. *Physica C* **2001**, *350*, 24.

(20) Choy, J. H.; Hwang, S. J.; Park, N. G. *J. Am. Chem. Soc.* **1997**, *119*, 1624.

(21) Lattice parameters of $RuSr_2GdCu_2O_8$: $a = 3.8412$ Å, $c = 11.5883$ Å, and $V = 170.9815$ Å^3. Lattice parameters of $RuSr_{1.9}La_{0.1}GdCu_2O_8$: $a = 3.8437$ Å, $c = 11.5452$ Å, and $V = 170.5700$ Å^3.

(22) Shannon, R. D. *Acta Crystallogr., Sect. A* **1976**, *32*, 751.

(23) Choy, J. H.; Kim, D. K.; Hwang, S. H.; Demazeau, G. *Phys. Rev. B* **1994**, *50*, 16631.

(24) Considering the fact that square pyramidal CuO_5 geometry in $RuSr_2GdCu_2O_8$ is an intermediate symmetry between octahedral CuO_6 geometry in La_2CuO_4 and square planar CuO_4 geometry in Nd_2CuO_4, we were able to estimate the average Cu valence of the ruthenocuprates by measuring the shift of the pre-edge peak from the average peak position between La_2CuO_4 and Nd_2CuO_4.

(25) Choy, J. H.; Kim, D. K.; Hwang, S. H.; Park, J. C. *J. Am. Chem. Soc.* **1995**, *117*, 7556.

(26) The best-fitted residual F^2 factors ($=\Sigma\{k_3(\chi(k)_{calcd} - \chi(k)_{exptl})\}_2/(n - 1)$) for the Cu K-edge EXAFS data are 0.026 for $RuSr_2GdCu_2O_8$ and 0.092 for $RuSr_{1.9}La_{0.1}GdCu_2O_8$.

(27) The Debye−Waller factors for the Cu−Sr/La shell were found to be rather larger than those for the other shells, which is attributable to the tilting of RuO_6 octahedra with respect to the *c*-axis, leading to the splitting of the Cu−Sr/La bond distances.

(28) The best-fitted residual F^2 factors ($=\Sigma\{k_3(\chi(k)_{calcd} - \chi(k)_{exptl})\}_2/(n - 1)$) for the Ru K-edge EXAFS data are 0.041 for $RuSr_2GdCu_2O_8$ and 0.045 for $RuSr_{1.9}La_{0.1}GdCu_2O_8$.

(29) Cao, G.; McCall, S.; Crow, J. E.; Guertin, R. P. *Phys. Rev. B* **1997**, *56*, R5740.

(30) Itoh, M.; Shikano, M.; Shimura, T. *Phys. Rev. B* **1995**, *16*, 16432.

(31) Battle, P. D.; Jones, C. W. *J. Solid State Chem.* **1989**, *78*, 108.

(32) Kumagai, K.; Takada, S.; Furukawa, Y. *Phys. Rev. B* **2001**, *63*, 180509.